JCI insight

RESEARCH ARTICLE

Adoptively transferred Vγ9Vδ2 T cells show potent antitumor effects in a preclinical B cell lymphomagenesis model

Nicholas A. Zumwalde,[1] Akshat Sharma,[1] Xuequn Xu,[1] Shidong Ma,[2] Christine L. Schneider,[3] James C. Romero-Masters,[2] Amy W. Hudson,[3] Annette Gendron-Fitzpatrick,[4] Shannon C. Kenney,[2] and Jenny E. Gumperz[1]

[1]Department of Medical Microbiology and Immunology, [2]Department of Oncology, University of Wisconsin School of Medicine and Public Health, Madison, Wisconsin, USA. [3]Department of Microbiology and Molecular Genetics, Medical College of Wisconsin, Milwaukee, Wisconsin, USA. [4]Comparative Pathology Laboratory, Research Animal Resources Center, University of Wisconsin School of Medicine and Public Health, Madison, Wisconsin, USA.

A central issue for adoptive cellular immunotherapy is overcoming immunosuppressive signals to achieve tumor clearance. While γδ T cells are known to be potent cytolytic effectors that can kill a variety of cancers, it is not clear whether they are inhibited by suppressive ligands expressed in tumor microenvironments. Here, we have used a powerful preclinical model where EBV infection drives the de novo generation of human B cell lymphomas in vivo, and autologous T lymphocytes are held in check by PD-1/CTLA-4–mediated inhibition. We show that a single dose of adoptively transferred Vδ2$^+$ T cells has potent antitumor effects, even in the absence of checkpoint blockade or activating compounds. Vδ2$^+$ T cell immunotherapy given within the first 5 days of EBV infection almost completely prevented the outgrowth of tumors. Vδ2$^+$ T cell immunotherapy given more than 3 weeks after infection (after neoplastic transformation is evident) resulted in a dramatic reduction in tumor burden. The immunotherapeutic Vδ2$^+$ T cells maintained low cell surface expression of PD-1 in vivo, and their recruitment to tumors was followed by a decrease in B cells expressing PD-L1 and PD-L2 inhibitory ligands. These results suggest that adoptively transferred PD-1^{lo} Vδ2$^+$ T cells circumvent the tumor checkpoint environment in vivo.

Introduction

γδ T cells are attractive candidates for adoptive immunotherapy in human cancer patients because they mediate potent antitumor effects in an MHC-independent manner (1–4), and therefore they do not require HLA matching of donors and recipients. Physiologically, γδ T cells are thought to be important for immunosurveillance (i.e., eradication of nascently transformed cells), since they can recognize early danger signals associated with neoplastic changes (5, 6). However, their role in controlling established tumors is not clear, as recent studies have identified tumor-infiltrating γδ T cells that appear to have protumorigenic functions (7, 8). Critical questions about the use of γδ T cells as agents of cellular immunotherapy thus involve understanding whether their ability to control cancers is subject to changes associated with tumor maturation, including whether their activating ligands are maintained or downregulated during the progression of tumorigenesis, and whether their responses are controlled by suppressive ligands that become upregulated during tumorigenesis.

Human γδ T cells are divided into 2 main subsets based on whether their T cell receptors (TCRs) use the Vδ1 or Vδ2 chain. Vδ1$^+$ T cells are mainly found in epithelial tissues, while most of the γδ T cells in human blood use the Vδ2 chain in combination with the Vγ9 chain (9). The mechanisms responsible for activating Vδ2$^+$ T cells are better understood than those of Vδ1$^+$ T cells, and therefore the Vδ2$^+$ subset has been more extensively investigated for immunotherapy. Functional responses of Vδ2$^+$ T cells can be initiated by at least 3 distinct recognition pathways: (a) via the TCR, (b) via natural killer (NK) family receptors such as NKG2D, and (c) via Fc receptor (CD16) binding to antibody-coated target cells (10). Each of these pathways may facilitate their antitumor responses.

TCR responses of Vδ2$^+$ cells depend on target cell expression of a highly conserved cell surface protein called butyrophilin 3A1 (BTN3A1), which is normally expressed in all tissues (11, 12). However, Vδ2$^+$

Authorship note: N.A. Zumwalde, A. Sharma, and X. Xu contributed equally to this work.

Conflict of interest: The authors have declared that no conflict of interest exists.

Submitted: February 1, 2017
Accepted: May 31, 2017
Published: July 6, 2017

Reference information:
JCI Insight. 2017;2(13):e93179.
https://doi.org/10.1172/jci.insight.93179.

TCRs only recognize the BTN3A1 molecule after it has undergone structural changes resulting from association with specific isoprenoid lipids (13–16). Isoprenoid lipids that activate Vδ2$^+$ T cells include prenylpyrophosphate metabolites that are produced by many bacterial species (17), as well as an intermediate of the mevalonate pathway called isopentenylpyrophosphate (IPP) that is produced by eukaryotic cells. Activity of the mevalonate pathway is often upregulated during neoplastic transformation, which in turn can result in greater accumulation of the IPP intermediate in cancer cells compared with normal cells. The presence of high levels of IPP appears to be a key factor in the ability of Vδ2$^+$ T cells to respond to human cancer cells in vitro (18). However, it is not clear whether endogenous expression levels of this metabolic intermediate are sufficient to permit immunotherapeutic Vδ2$^+$ T cells to target emerging or established cancers in vivo.

γδ T cells may also specifically target tumors in a TCR-independent manner through recognition of innate ligands. Vδ2$^+$ T cells express an activating receptor of the NK complex called NKG2D. This is a transmembrane C-type lectin that recognizes at least 8 different ligands, including the MHC class I–related chain (MIC) A and B molecules, and a family of related molecules called UL16-binding protein (ULBP) 1–6 (19). Expression of MICA/B and ULBP molecules is increased under conditions of stress (e.g., microbial infection, hyperproliferation, and neoplastic transformation), and many tumors express elevated levels of these ligands at the cell surface (20). NKG2D-mediated recognition of MICA/B molecules markedly costimulates TCR-dependent effector responses of Vδ2$^+$ T cells, and may also be sufficient to activate them in a TCR-independent manner (21–23). However, ligands recognized by NKG2D can be downregulated from the cell surface by tumor cells and secreted in a soluble form as a mechanism of immune evasion or suppression (24), and therefore the use of this recognition pathway for immunotherapy must be carefully evaluated.

Preclinical in vivo modeling is thus key to understanding how to design effective immunotherapy strategies using human γδ T cells. However, a challenge to modeling the actions of human Vδ2$^+$ T cells in vivo is that rodents do not possess a similar isoprenoid-reactive γδ T cell subset, and lack the BTN3A1 isoform (25, 26). Prior studies have thus xenografted established human tumors into immune-deficient mice in the presence or absence of human Vδ2$^+$ T cells to evaluate their effects in vivo (27–32). These studies have provided important demonstrations of the antitumor potential of human Vδ2$^+$ T cells. However, studies of this kind do not capture the dynamic changes associated with the process of tumorigenesis, and in particular may not model how the upregulation of immunosuppressive ligands by tumors, which is accompanied by the presence of anergized T lymphocytes, affects the success of cellular immunotherapy.

Here we have used a powerful model in which Epstein-Barr virus (EBV) drives human B cells to transition from healthy cells into lymphomas over the course of several weeks in vivo. EBV is a human-specific γ-herpesvirus that is associated with several types of human B cell lymphoma, including Burkitt lymphoma, Hodgkin lymphoma, diffuse large B cell lymphoma, and posttransplant lymphoproliferative disease (33). A key feature of our model system is that neoplastic transformation of the human B cells occurs in the presence of autologous human T lymphocytes (34). Importantly, the autologous T cells are held in check by PD-1 and CTLA-4, which limit their ability to control the B lymphomas (35). This system therefore allowed us to test the effects of Vδ2$^+$ T cell adoptive immunotherapy in vivo before and after the establishment of tumor masses, and in the context of tumor-suppressive ligands.

Results

De novo lymphomagenesis. To induce the formation of human B cell lymphomas in vivo, we briefly incubated human umbilical cord blood mononuclear cells (CBMCs) with EBV in vitro to allow viral attachment to the B cells, and then injected the human cells intraperitoneally into NSG mice (34). Using this protocol, typically about 90% of the mice develop tumors that result in mortality within 5 weeks (Figure 1A). Histological analysis revealed that by 14 days after injection, lymphoid aggregates are apparent in the fatty tissue near the pancreas. The aggregates include cells expressing the EBV nuclear antigen 1 (EBNA1), indicating that virally infected cells are present, but at this stage signs of neoplastic transformation are not apparent (Figure 1B). However, by 21 days after injection the lymphoid aggregates do show signs of neoplasia, including the presence of mitotic figures, areas of necrosis, and apoptotic debris (Figure 1B). By 28 days after injection, the lymphoid masses have expanded dramatically and typically appear to have started invading nearby organ tissue (Figure 1B). Based on these results, administration of cellular immunotherapy during the first week after injection of the EBV-treated CBMCs will likely assess immunosurveillance effects (i.e., clearance of EBV-infected cells prior to generation of a tumor microenvironment), whereas administering the immunotherapy later than 3 weeks after injection will assess the impact on established tumors.

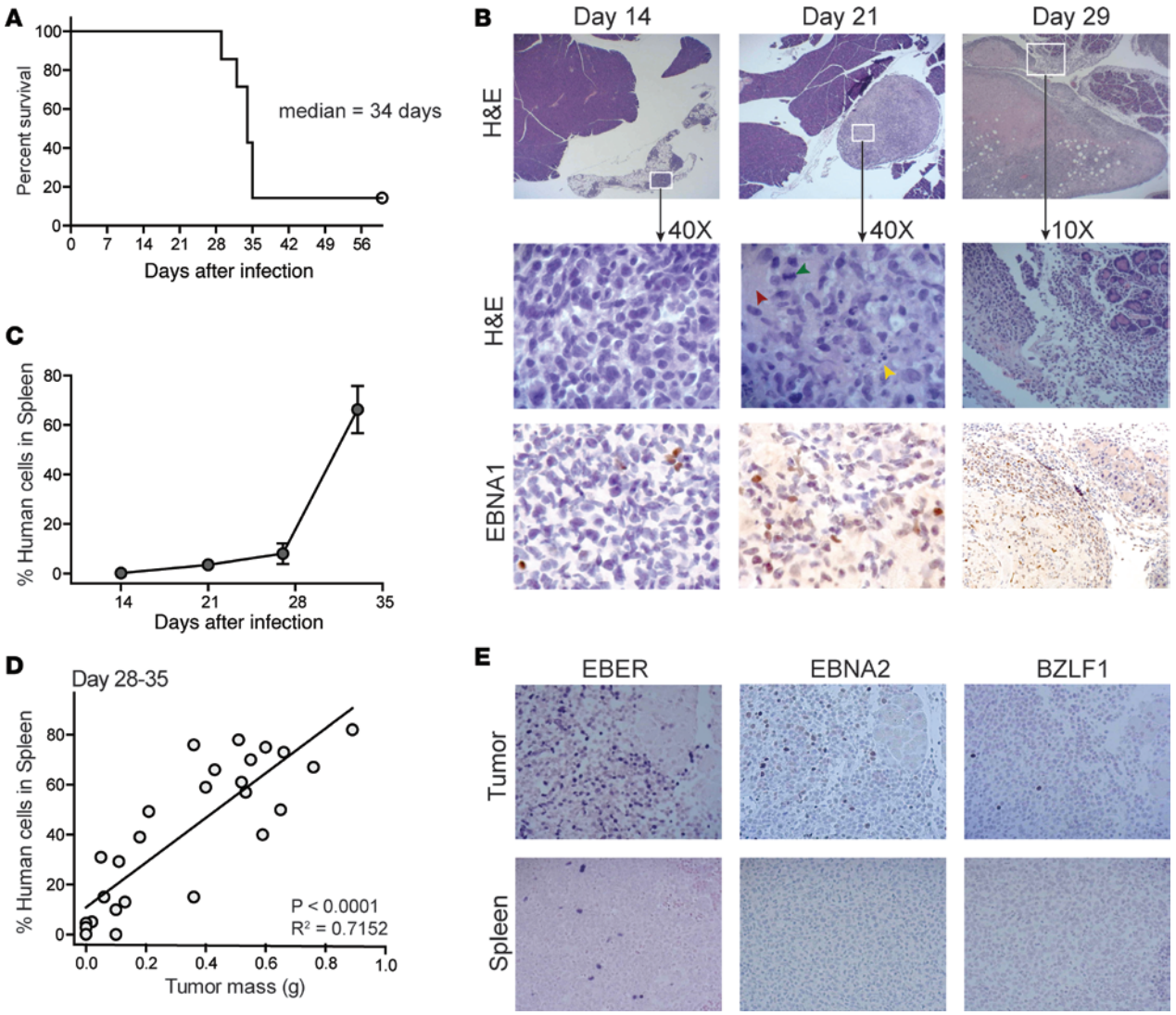

Figure 1. Model of human EBV-driven lymphomagenesis. Human umbilical cord blood mononuclear cells (CBMCs) were exposed to EBV for 2 hours in vitro and then washed, and 10 × 10^6 cells per mouse were injected intraperitoneally into NSG mice. (**A**) Survival results from a representative experiment with 7 mice; similar results were obtained in a second independent experiment. (**B**) Histological analyses of peri-pancreatic tissue taken at the indicated times after injection of the human cells. Top row shows low magnification (×2) H&E–stained images revealing the growth of lymphoid masses near pancreatic tissue. Middle row shows higher magnification of the indicated areas; neoplastic changes are visible at the day 21 time point, including areas of necrosis (red arrowhead), apoptotic debris (yellow arrowhead), and mitotic figures (green arrowhead). The bottom row shows IHC staining to detect expression of the EBNA1 viral protein (visualized with diaminobenzidine, brown color). The sections are counterstained with hematoxylin (blue color). (**C**) Frequency of human cells in spleen as determined by flow cytometric analysis of total splenocytes at the indicated time points. Each symbol represents the mean frequency from 3 different mice; error bars (not always visible on this scale) show the standard deviations. (**D**) The frequency of human cells in spleen was plotted against the total mass of tumor tissue excised from the peritoneal cavity for each mouse. Results are from mice sacrificed between 28 and 35 days after injection of EBV-treated CBMCs. Statistical results from a linear regression analysis are shown in the bottom-right corner of the plot. (**E**) Histological analyses for indicators of EBV infection from tumor tissue (top row) and spleen tissue (bottom row) at ×20 magnification. Left panels show in situ hybridization for EBV-encoded small RNAs (EBER, indicated by dark purple color); middle and right panels show IHC staining for the EBV proteins EBNA2 and BZLF1, respectively (positive cells have dark nuclei).

Spleen appears protected from tumorigenesis. Analysis of human cells in the spleens of mice engrafted with EBV-treated CBMCs consistently showed that there was a slow increase in human cell frequency between 14 and 28 days after injection, followed by a rapid rise between day 28 and 35 (Figure 1C). There was a clear correlation between the frequency of human cells in the spleen and the mass of the peritoneal tumors during the day 28–35 time window (Figure 1D), suggesting that tumorigenesis is associated with expansion of human cells in the spleen. However, unlike lymphoid masses in the peritoneal cavity, there was no histological evidence of neoplasia in the spleen (data not shown). Tumors in the peritoneal cavity contained abundant cells expressing EBV-encoded small RNAs (EBERs), as well as proteins associated with type-III EBV latency (EBNA2) and

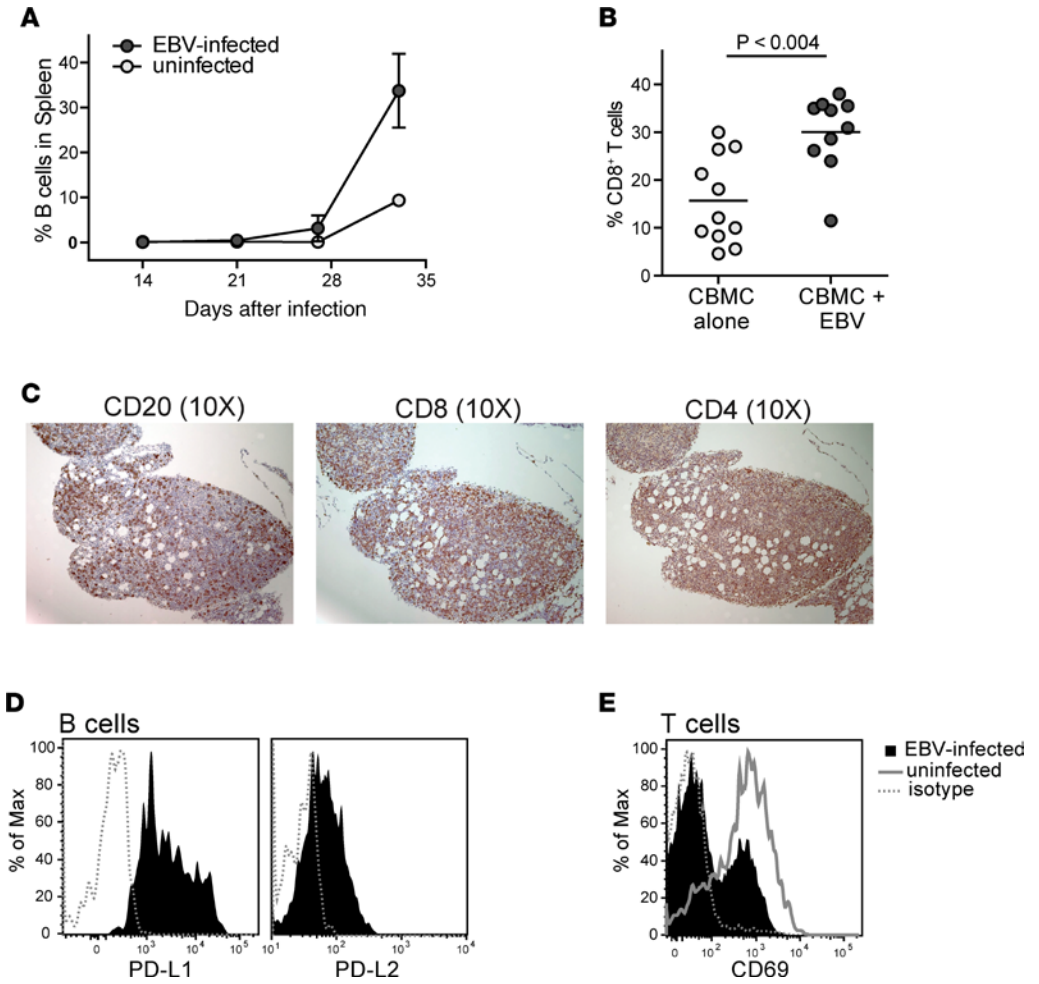

Figure 2. Autologous T cells are expanded during EBV infection. NSG mice were injected with 10 × 10^6 EBV- or mock-treated (uninfected) human umbilical cord blood mononuclear cells (CBMCs). (**A**) Plot showing the percentage of the human cells from spleen that stained positively for the B cell marker CD19 at the indicated time points after injection. Each data point represents the mean from 3 different mice; error bars (not always visible on this scale) show the standard deviations. (**B**) Percentage of $CD8^+$ T cells of the human cells in spleens harvested between 26 and 35 days after injection. Each data point shows the results from an individual mouse. The *P* value was calculated using a 2-tailed nonparametric *t* test (Mann-Whitney analysis). (**C**) IHC of serial sections of a peritoneal tumor taken at 3 weeks after injection of EBV-treated CBMCs. Brown color shows staining for human CD20 (left), human CD8 (middle), and human CD4 (right); hematoxylin counterstaining shows cell nuclei (blue color). (**D**) Flow cytometric analysis of tumor B cells for PD-L1 (left) and PD-L2 (right). Filled histograms show staining by specific mAbs, dotted line shows staining by an isotype control mAb. (**E**) Flow cytometric analysis of splenic T cells from an EBV-infected mouse for expression of the activation marker CD69 (filled histogram) compared to an isotype control mAb (dotted line); the solid gray line shows CD69 staining of splenic T cells from an uninfected mouse.

lytic replication (BZLF1) (Figure 1E), suggesting a high level of viral transforming activity in the tumors. In contrast, the spleen showed only sparse EBER staining and little or no positive staining for EBNA2 or BZLF1. Thus, although virally infected cells are present in the spleen, they are likely in a deeper state of latency, and neoplastic transformation resulting in the formation of tumors is limited or absent at this location.

Expansion of autologous T cells during EBV infection. The human CBMC samples used to engraft the mice for these studies typically contain less than 10% B lymphocytes, while about 60% of the cells are T lymphocytes (data not shown). Exposing the CBMCs to EBV leads to a marked expansion of the B lymphocytes by about 28 days after injection (Figure 2A). Analysis of human T cells in the spleen revealed significantly higher proportions of $CD8^+$ T cells in EBV-infected mice compared with noninfected controls (Figure 2B), suggesting that cytotoxic T lymphocytes (CTLs) are expanded in response to the viral infection. Moreover, histological analyses revealed that in addition to containing B lymphocytes, the tumors in these mice are also highly infiltrated by $CD8^+$ and $CD4^+$ T cells (Figure 2C). However, as we showed in a previous publication (35), the tumor B cells express inhibitory ligands such as PD-L1 and PD-L2 (Figure 2D), and this results in the autologous T cells being held in check. Consistent with the

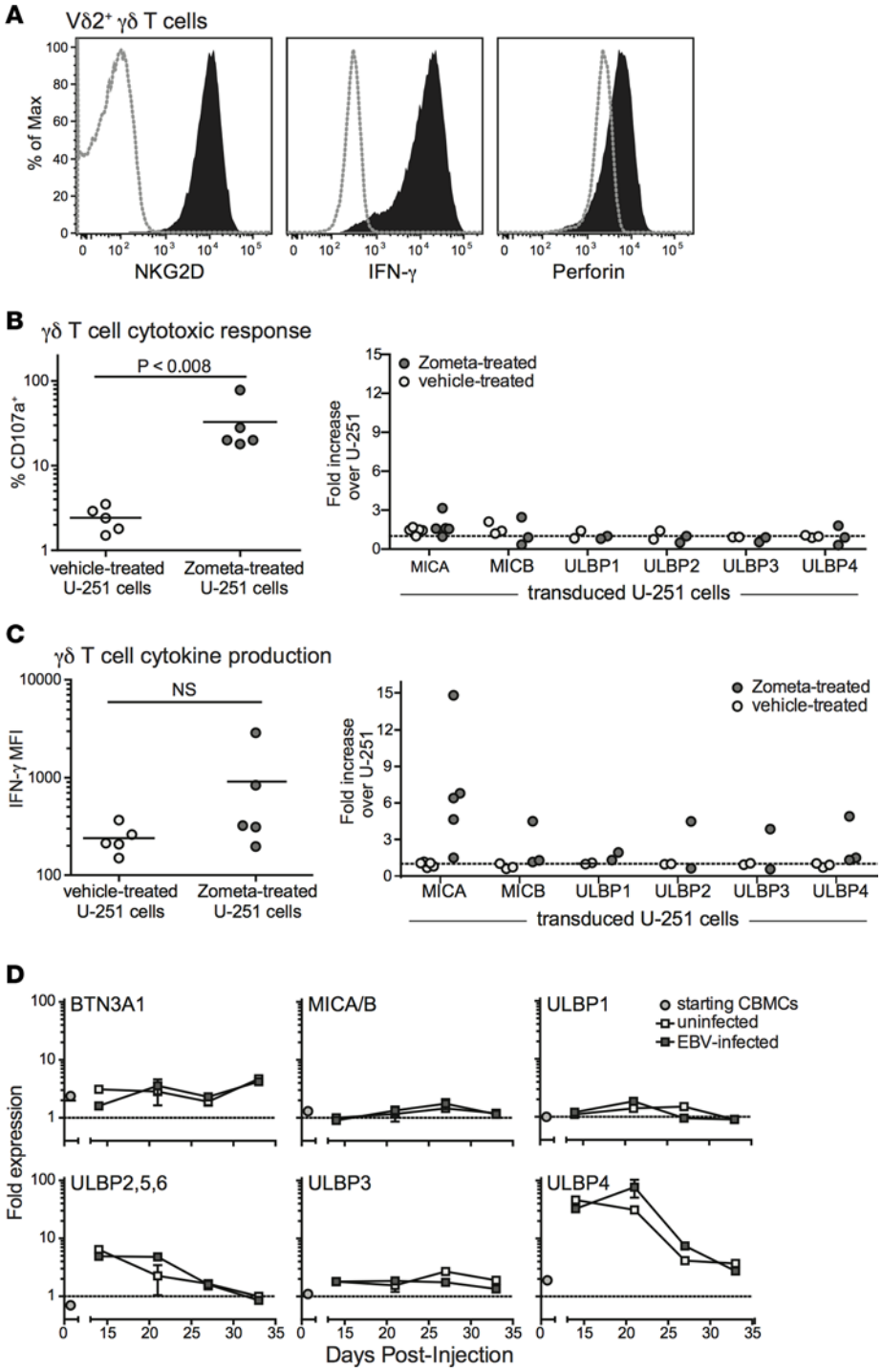

Figure 3. Analysis of TCR- and NKG2D-mediated Vδ2⁺ T cell responses. Vδ2⁺ T cells were expanded in vitro from adult human peripheral blood mononuclear cells by exposure to zoledronic acid (Zometa). (**A**) Flow cytometric analysis of the Vδ2⁺ T cells for cell surface expression of NKG2D, intracellular IFN-γ, and intracellular perforin (filled histograms). Dotted lines show staining with isotype-matched negative control mAbs. (**B**) The γδ T cell cultures were exposed for 4 hours to U-251 glioblastoma cells that were pretreated with Zometa to induce accumulation of isopentenylpyrophosphate, or mock-treated, and Vδ2⁺ T cell surface CD107a expression was assessed by flow cytometry. Left plot shows aggregated results from 5 independent experiments comparing the percentage of CD107a-positive cells in response to parental U-251 cells that express BTN3A1 but have little or no expression of NKG2D ligands. Right plot shows γδ T cell responses to U-251 transductants expressing the indicated NKG2D ligands; the percentage of CD107a⁺ Vδ2⁺ T cells responding to each transductant was normalized by the response to the parental U-251 cells. (**C**) Intracellular IFN-γ staining results from the experiments described in **B**. (**D**) Flow cytometric analysis was performed on uninfected human umbilical cord blood mononuclear cells (CBMCs) (circles), or on splenic B cells taken from mice given uninfected or EBV-treated CBMCs (light or dark gray squares, respectively) at the indicated times after injection. The cell surface expression of the indicated ligands is given as the median fluorescence intensity (MFI) obtained with the relevant specific mAb normalized by that from an isotype-matched negative control. Data points represent the mean values obtained from 1–4 separate analyses. NS, not significant.

presence of an inhibitory environment, we observed that T cells from tumor-bearing mice typically show less expression of the CD69 activation marker than their counterparts from mice engrafted with noninfected CBMCs (Figure 2E). Thus, this experimental model recapitulates an important hallmark of many cancers: endogenous T cells are present, but they are held in a suppressed state.

Characteristics of γδ T cells used for immunotherapy. Vγ9Vδ2⁺ T cells were expanded by culturing peripheral blood mononuclear cell (PBMC) samples from healthy adults in medium containing 2.5 μM zoledronic acid (Zometa) and 200 U/ml recombinant human IL-2 for 7–14 days, as previously described (36). Aminobisphosphonate drugs such as Zometa stimulate Vδ2⁺ T cell proliferation in a dose-dependent manner, because they block the mevalonate biosynthesis pathway and cause the accumulation of IPP, which then associates with BTN3A1 and is recognized by the TCR (11, 12). After this treatment, the PBMC cultures typically consisted of 80%–90% γδ T cells (Supplemental Figure 1; supplemental material available online with this article; https://doi.org/10.1172/jci.insight.93179DS1). Flow cytometric analysis confirmed that the expanded γδ T cells express the innate receptor NKG2D, and produce both IFN-γ and the cytolytic protein perforin (Figure 3A).

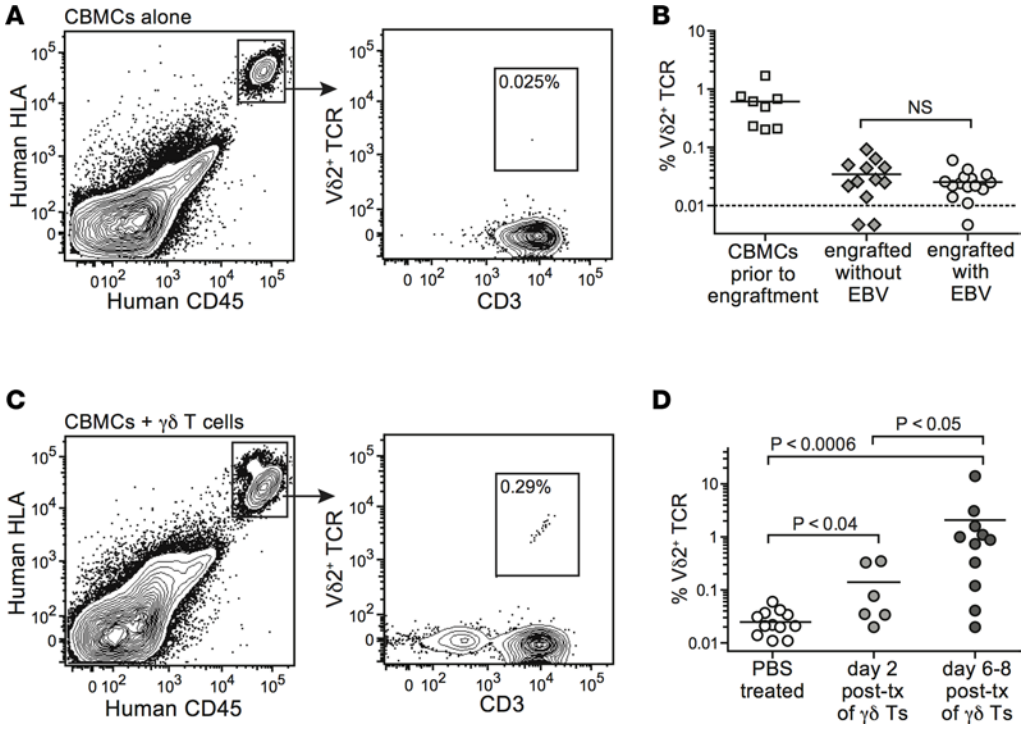

Figure 4. Vδ2⁺ T cells from engrafted cord blood do not expand in vivo in response to EBV infection, but adoptively transferred Vδ2⁺ T cells persist for at least 1 week. (**A**) Flow cytometric staining for human Vδ2⁺ T cells in the spleen of a representative mouse engrafted with human umbilical cord blood mononuclear cells (CBMCs) alone. (**B**) Aggregated results showing the percentage of T cells expressing a Vδ2⁺ TCR in starting CBMC samples compared with the percentage detected in spleens of CBMC-engrafted mice in the presence or absence of EBV infection. (**C**) Flow cytometric staining for human Vδ2⁺ T cells in the spleen of a representative CBMC-engrafted mouse that received adoptively transferred γδ T cells. (**D**) Aggregated results showing the percentage of Vδ2⁺ T cells in spleens of CBMC-engrafted mice given PBS (mock treatment) or in vitro–expanded γδ T cells. Spleens were harvested at the indicated times following administration of PBS or γδ T cells. *P* values were calculated using a 2-tailed nonparametric *t* test (Mann-Whitney analysis). NS, not significant; tx, transfer.

Prior studies have indicated that Vδ2⁺ T cells can respond to target cells via both TCR- and NKG2D-dependent mechanisms (21–23, 37, 38). To investigate the role of TCR- and NKG2D-mediated recognition in activating cytotoxic and cytokine responses by our expanded γδ T cells, we used a human glioblastoma cell line called U-251 MG. This cell line expresses low, but detectable levels of BTN3A1 at the cell surface, lacks detectable MICA and MICB, and has only minimal surface expression of ULBP molecules (Supplemental Figure 2). The γδ T cells were incubated with U-251 cells that were pretreated with vehicle alone or with Zometa, and T cell surface expression of CD107a (an indicator of recent cytolytic activity) was assessed by flow cytometry. Exposure to U-251 cells that had been sensitized with Zometa efficiently stimulated CD107a expression by the γδ T cells, whereas exposure to vehicle-treated U-251 cells induced very little CD107a upregulation (Figure 3B). Since Zometa sensitization exclusively impacts TCR-mediated recognition, these results indicate that cytotoxic responses by the expanded γδ T cells are activated by TCR stimulation. Notably, exposing the γδ T cells to retrovirally transduced U-251 cell lines that express high levels of individual NKG2D ligands did not lead to increased CD107a expression (Figure 3B), suggesting that costimulation by NKG2D does not enhance their cytotoxic responses. In contrast, a parallel analysis of IFN-γ production by the expanded γδ T cells suggested that target cell expression of NKG2D ligands can markedly costimulate cytokine production (Figure 3C).

To gain further insight, we assessed B cell expression of TCR and NKG2D ligands in our model system. The BTN3A1 glycoprotein was detectable on B cells in the CBMC samples used for engraftment, and its expression was maintained at similar levels following injection into NSG mice, regardless of whether the cells were exposed to EBV or not (Figure 3D). B cells in the starting CBMC sample showed little or no expression of NKG2D ligands (MICA/B, or ULBP1–6), and MICA/B molecules did not appear to become significantly upregulated after injection into the mice (Figure 3D). While 2 ULBP isoforms (ULBP2,5,6 and ULBP4) did show marked upregulation after transfer, this was not specific to the EBV-exposed cells. These results suggested that TCR-mediated pathways are available for activating γδ T cells in this model, but that NKG2D-mediated pathways are limited.

Detection of γδ T cells in vivo. The T cell compartment of human CBMC samples typically contains about 0.5%–2% Vδ2⁺ T cells (39). We investigated the frequencies of Vδ2⁺ cells within the human T cell compartment in spleens of mice engrafted with EBV-infected or uninfected CBMCs. Human cells in the murine spleens were readily delineated using mAbs specific for human HLA class I and human CD45 (Figure 4A). Analyses of splenocytes harvested 2–4 weeks after CBMC engraftment revealed only very low, or in some

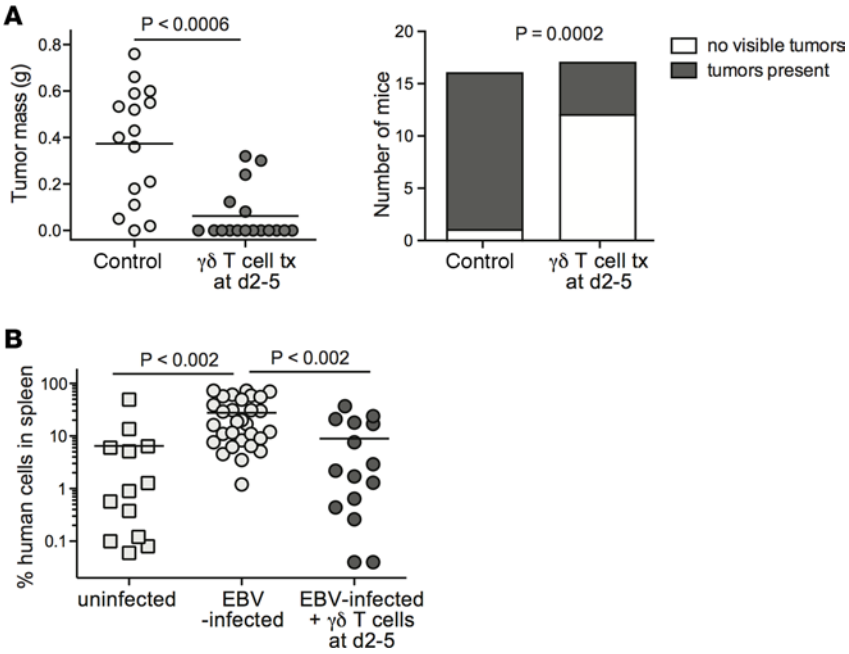

Figure 5. Early γδ T cell immunotherapy prevents tumor outgrowth and EBV-driven expansion of human cells in spleen. NSG mice were injected intraperitoneally with 10×10^6 EBV-treated human umbilical cord blood mononuclear cells (CBMCs). After 2–5 days, the mice were intravenously injected with a single dose of 5×10^6 to 10×10^6 γδ T cells, or not treated (control). Tumor and spleen tissues were harvested between 28 and 35 days after injection of the EBV-treated CBMCs, depending on when the control mice from the experiment appeared moribund. (**A**) Plots showing aggregated results from 3 independent experiments. Left plot shows tumor masses with each data point representing an individual mouse; the *P* value was calculated using a stratified nonparametric 2-tailed test (van Elteren analysis). Right plot shows the number of mice in each treatment group that had macroscopically visible tumor tissue, regardless of tumor mass; the *P* value was calculated using a 2-sided Fisher's exact *t* test. (**B**) Aggregated results from flow cytometric analysis showing the frequency of human cells in spleens of mice given mock-treated CBMCs (uninfected), or EBV-treated CBMCs with no immunotherapy (EBV-infected), or EBV-treated CBMCs followed by γδ T cells 2–5 days later. Each data point represents the result from an individual mouse. *P* values were calculated using a 2-tailed nonparametric *t* test (Mann-Whitney analysis). tx, transfer.

cases undetectable, frequencies of Vδ2$^+$ T cells (Figure 4, A and B). EBV infection did not result in increased Vδ2$^+$ T cell frequencies (Figure 4B). In contrast, flow cytometric analyses of CBMC-engrafted mice that were adoptively transferred with 1×10^6 to 5×10^6 in vitro–expanded γδ T cells consistently revealed a small but readily detectable population in the spleen (Figure 4C). Human Vδ2$^+$ T cells were detectable in spleens for at least 1 week after adoptive transfer, and their frequency appeared to increase somewhat during this time (Figure 4D), suggesting that they were not being rapidly eliminated by T cells derived from the CBMC sample.

Effects of γδ T cell immunotherapy. We investigated the impact of adoptive transfer of in vitro–expanded γδ T cells on the size and incidence of EBV-induced tumors. NSG mice were injected with EBV-exposed CBMCs and then given a single dose of γδ T cells 2–5 days later. This treatment had a significant impact on tumor outgrowth ($P < 0.0006$), with the majority of the γδ T cell–treated mice failing to develop macroscopically detectable tumors (Figure 5A). We also observed that the EBV-associated expansion of human cells in the spleen did not occur in mice that received γδ T cells within 1 week (Figure 5B), indicating that the effects of the γδ T cells are not limited to peritoneal sites of tumorigenesis. Thus, early time point γδ T cell therapy had effects that appeared consistent with immunosurveillance.

We next investigated the impact of administering γδ T cell therapy at later time points, after neoplastic changes to lymphoid masses in the peritoneal cavity are typically apparent. NSG mice were injected with EBV-exposed CBMCs, and injected with a single dose of γδ T cells or vehicle (sterile PBS) 22–25 days later. The mice were sacrificed 5–7 days after administration of the immunotherapy, and peritoneal tissue was collected for analysis. Compared with the vehicle-treated mice, those that received γδ T cells showed significantly reduced peritoneal tumor mass ($P < 0.00002$) (Figure 6A). Notably, this single-dose, late time point immunotherapy protocol did not usually result in a complete eradication of tumor tissue (Figure 6B).

PD-1 expression of adoptively transferred γδ T cells. We have recently shown that the administration of checkpoint-blockade antibodies (anti–PD-1 and anti-CTLA4) results in reduced tumor burden and enhanced survival in this model (35). Together with additional findings (e.g., that checkpoint inhibition was associated with improved EBV antigen–specific IFN-γ secretion by T cells from EBV-infected mice), these results suggested that antitumor T cell responses are usually held in check by inhibitory ligands in this model. Based on these prior observations, we were surprised at the dramatic antitumor effects of γδ T cells that were administered without additional measures to provide checkpoint blockade. However, flow cytometric analysis of splenic T cells from adoptively transferred mice revealed that the γδ T cell subset showed very low PD-1 expression compared with CD8$^+$ T cells and most of the CD4$^+$ T cells (Figure 7A). Thus, low PD-1 expression might be key to the antitumor efficacy of immunotherapeutic γδ T cells, but the stability of this state was not clear.

To further investigate, we assessed PD-1 expression by γδ T cells in adult human PBMC samples directly ex vivo, and at a series of time points during our in vitro expansion protocol. There was little cell surface

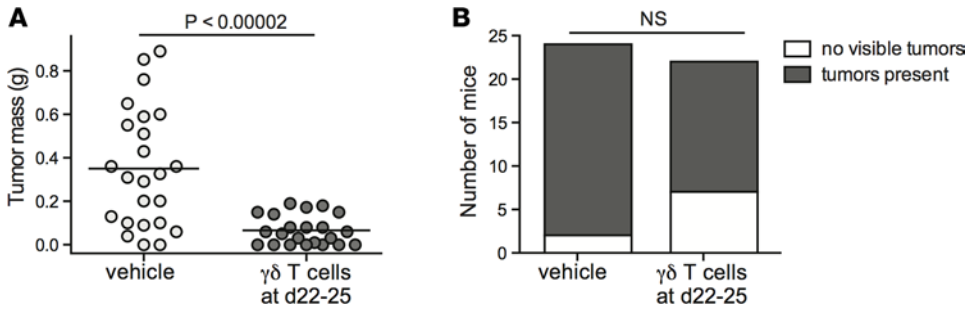

Figure 6. Administration of γδ T cell immunotherapy after onset of neoplastic transformation limits tumor size. NSG mice were injected intraperitoneally with 10×10^6 EBV-treated human umbilical cord blood mononuclear cells (CBMCs). After 22–25 days, the mice were intravenously injected with a single dose of 5×10^6 to 10×10^6 γδ T cells or sterile PBS (vehicle). (**A**) Plot showing aggregated results of tumor mass from 4 independent experiments, with each data point representing an individual mouse; the *P* value was calculated using a stratified nonparametric 2-tailed test (van Elteren analysis). (**B**) Plot showing the number of mice in each treatment group that had macroscopically visible tumor tissue, regardless of tumor mass. NS, not significant based on a 2-sided Fisher's exact *t* test.

PD-1 on Vδ2$^+$ T cells in the starting PBMC samples, but the expression of this ligand was markedly upregulated over the first 4 days of exposure to Zometa in vitro (Figure 7B). However, thereafter the PD-1 expression levels dropped, and by 7 days of in vitro expansion (the time at which the γδ T cell frequency in the culture typically reaches its maximum) the PD-1 expression had returned nearly to baseline (Figure 7B).

We next tested the impact of adoptive transfer into CBMC-engrafted mice on the expression of PD-1 by in vitro–expanded γδ T cells. A PBMC sample that stained positively for HLA-A2 was cultured with Zometa for varying lengths of time, and then 5×10^6 cultured cells per mouse were injected intravenously into NSG mice that had been engrafted 3 weeks earlier with an HLA-A2–negative CBMC sample. Five days after the adoptive transfer, splenocytes were harvested and PD-1 expression levels were assessed on HLA-A2$^+$ γδ T cells. As shown in Figure 7C, PD-1 expression levels on the splenic γδ T cells after 5 days in vivo closely matched the PD-1 expression levels present on the γδ T cells at the time they were injected. Thus, the initial level of PD-1 expression on adoptively transferred γδ T cells appeared to be maintained in vivo.

Finally, we performed an experiment to compare PD-1 expression by adoptively transferred γδ versus αβ T cells. A PBMC sample that stained positively for HLA-A2 was expanded for 8 days with a slightly suboptimal concentration of Zometa, resulting in a mixed culture of 67% γδ and 33% αβ T cells. These cells were injected into EBV-infected mice engrafted with HLA-A2–negative CBMCs. CBMC-derived and adoptively transferred T cells in the spleens of the mice were analyzed by flow cytometry for PD-1 expression levels (Figure 7D). The adoptively transferred γδ T cells consistently showed lower PD-1 expression than the transferred αβ T cells, while the CBMC-derived T cells showed very high PD-1 expression (Figure 7E). Together, these results underscore the selectivity of low PD-1 expression by our immunotherapeutic γδ T cells.

Analysis of tumors after late γδ T cell treatment. Histological analyses of tissue slides from γδ T cell–treated mice frequently showed CD3$^+$ cells that localized to areas of the tumors containing high frequencies of cells expressing the EBV protein EBNA2 (Figure 8A). Interestingly, however, careful inspection of tumor sections often revealed the presence of CD3$^+$ cells in the lumens of blood vessels within the tumors (Figure 8A), suggesting active trafficking of T cells. Flow cytometric analyses of the frequency of γδ T cells found in spleen and tumor tissues from the same mice suggested there was a trend towards increased γδ T cell representation in tumors compared with spleens (Figure 8B). Moreover, using HLA-A2 expression to specifically track the adoptively transferred population, we observed that at 2 days after injection of a mixed population of αβ and γδ T cells (67% γδ, 33% αβ), the transferred γδ T cells appeared significantly more enriched in the tumor tissue than the transferred αβ T cells. In contrast, in the spleen the proportion of adoptively transferred γδ versus αβ T cells was close to that of the initial mixture (Figure 8B).

Further flow cytometric analysis revealed that mice that received late time point γδ T cell immunotherapy had B cell frequencies similar to those of mock-treated mice at 2–3 days after transfer, but by 5–8 days after transfer there was a significant reduction in B cell frequency in tumors of γδ T cell–treated mice (Figure 8C). Additionally, the γδ T cell therapy appeared to be associated with reduced surface expression of PD-L1 and PD-L2 on tumor B cells, compared with those from vehicle-treated mice (Figure 8D). Together, these results suggested that although the adoptively transferred γδ T cells localized to both spleen and tumor

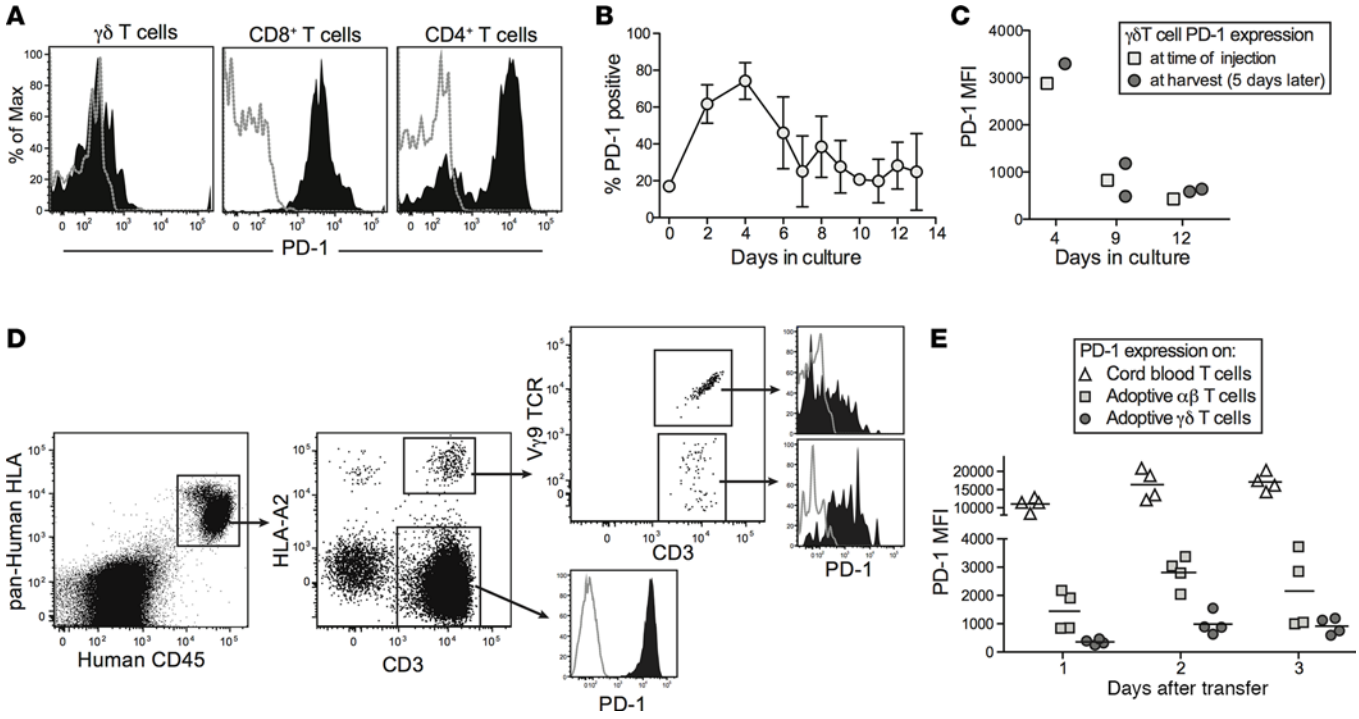

Figure 7. Low PD-1 expression maintained in vivo by adoptively transferred γδ T cells. (**A**) Analysis of PD-1 expression by human T cell subsets from an EBV-infected mouse that was administered γδ T cells that had been expanded in vitro for 8 days. Filled histograms show anti–PD-1 staining; gray dotted lines show staining by an isotype-matched control mAb. (**B**) Expression of PD-1 by Vδ2⁺ T cells over the course of in vitro expansion. Total human peripheral blood mononuclear cells freshly isolated from healthy adult donors were cultured in medium containing 2.5 μM zoledronic acid (Zometa), and expression of PD-1 on Vδ2⁺ T cells was assessed by flow cytometry at the indicated time points. Data points show the means and standard deviations of results from 3–5 independent experiments taken at the indicated time points. (**C**) Plot showing PD-1 expression by in vitro–expanded γδ T cells immediately prior to injection into human umbilical cord blood mononuclear cell–engrafted (CBMC-engrafted) NSG mice (squares) or at the time of harvest from spleens 5 days later (circles). Adoptively transferred γδ T cells were differentiated from the CBMCs used for engraftment by analysis of HLA-A2 expression, which was intentionally mismatched. (**D**) EBV-infected mice were administered a mixed population of αβ and γδ T cells (approximately 35% αβ and 65% γδ) obtained by culture with a suboptimal concentration of Zometa. Flow cytometric analysis of splenocytes showing PD-1 expression by the adoptively transferred T cells (HLA-A2 positive) segregated according to γδ TCR expression, compared with T cells from the CBMC sample that was used for the initial engraftment (HLA-A2 negative). (**E**) Plot showing PD-1 expression by the indicated splenic T cell populations from 4 separate mice.

tissue, in the first 2 days after injection the γδ T cells may tend to preferentially accumulate within tumors. At somewhat later time points (5–7 days after injection), γδ T cell therapy was associated with changes to the frequency and PD-L1/L2 phenotype of B cells in residual tumors.

Discussion

It is now clear that suppressive effects mediated by the upregulation of inhibitory B7 family members within tumor microenvironments are an important factor in the failure of cytolytic lymphocytes to control tumors (40, 41). A central issue for cellular immunotherapies is therefore avoiding inhibition of adoptively transferred cells by these pathways. We have recently shown that in our in vivo model of EBV-driven B lymphomagenesis, the antitumor effects of endogenous human T cells are limited by checkpoint inhibition mediated via PD-1 and CTLA-4 (35). Here, we show that adoptively transferred Vδ2⁺ T cells expanded from human PBMCs have potent antitumor effects, even without coadministering checkpoint inhibitors. Remarkably, after completing their most active phase of Zometa-induced expansion in vitro, the γδ T cells we used for immunotherapy show only low levels of PD-1 expression, and their PD-1^{lo} status is maintained after transfer into CBMC-engrafted NSG mice. These findings suggest an intriguing rationale for why the immunotherapeutic γδ T cells are able to mediate strong antitumor effects: they are likely less affected than the endogenous T cells by inhibitory ligands expressed by the tumor B cells. Thus, in addition to supporting the potential clinical utility of in vitro–expanded Vδ2⁺ T cells, our analysis suggests that a key area for future investigation will be to understand in detail the regulation of PD-1 expression on human γδ T cells that are to be used for cellular immunotherapy.

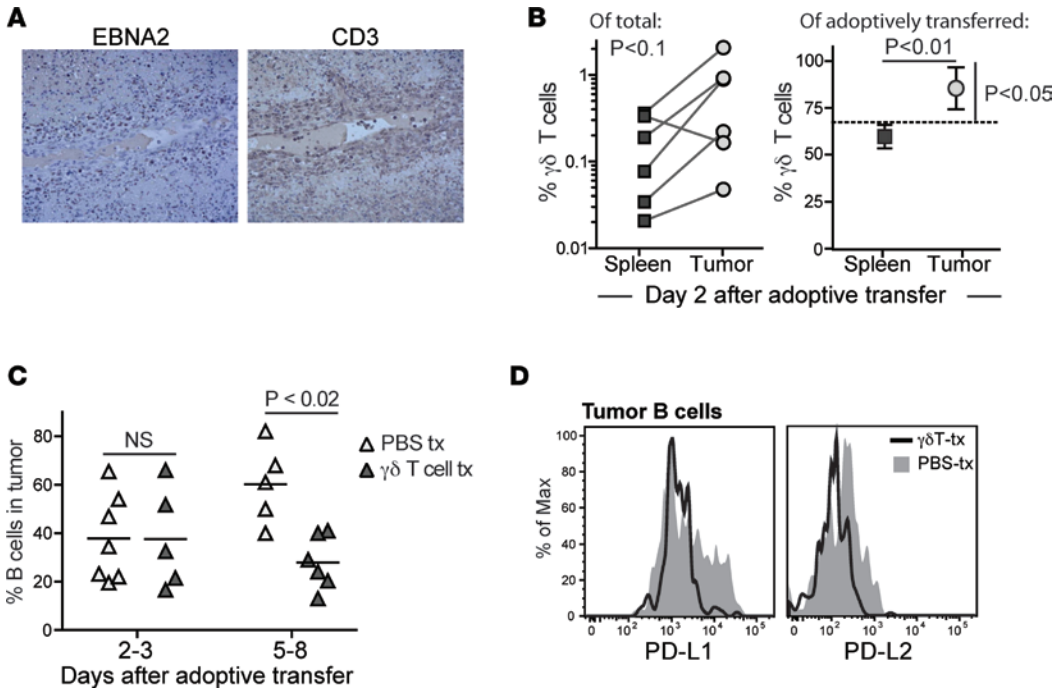

Figure 8. Recruitment of γδ T cells and analysis of tumor B cells after late time point γδ T cell administration. (**A**) Light microscopic images (×10 magnification) of IHC of serial sections of tumor tissue from a γδ T cell–treated mouse showing cells expressing the viral protein EBNA2 (left image) or CD3 (right image). T cells are observed within the blood vessel in the middle of the field, as well as infiltrating the surrounding tissue in areas where EBNA2$^+$ cells are localized. (**B**) Adoptively transferred γδ T cells appear slightly enriched in tumor tissue compared with spleen. Left plot: percentage of human T cells expressing Vδ2 in paired spleen versus tumor tissue samples from independent mice. Tissues were harvested 2 days after administration of γδ T cell immunotherapy. The *P* value was calculated using a paired, nonparametric *t* test (Wilcoxon signed-rank test). Right plot: percentage of the adoptively transferred cells in spleen versus tumor expressing a Vγ2Vδ2$^+$ TCR. The dashed line shows the frequency of γδ T cells in the injected population; symbols show mean and standard deviations of 4 replicate analyses each of spleen and tumor tissue. The *P* value comparing spleen versus tumor frequencies (horizontal line) was calculated using an unpaired parametric *t* test; the *P* value comparing tumor mean to the γδ T cell frequency of the injected cells (vertical bar) was calculated using a 1-sample, 2-tailed *t* test. (**C**) B cells as a percentage of the total human cells in tumor tissue from a series of mice that were administered γδ T cells (dark triangles) or vehicle (light triangles). Tumors were harvested at the indicated times after adoptive transfer or mock treatment. The *P* value was calculated using a 2-tailed nonparametric *t* test (Mann-Whitney analysis). (**D**) Flow cytometric analysis of PD-L1 and PD-L2 staining on tumor B cells. Filled gray histograms show results from a mouse given vehicle (PBS-tx); black line shows results from a mouse given γδ T cells. tx, transfer.

A study by Xiang et al. recently established that similar in vitro–expanded human Vδ2$^+$ T cells can control the growth in vivo of human B lymphoblastoid cell lines that were first transformed by EBV in vitro and then transferred into NSG mice (32). While providing a powerful demonstration that high doses of Vδ2$^+$ T cells are sufficient to kill EBV-transformed B lymphoblastoid cells in vivo, the analysis by Xiang et al. did not address the more physiological scenario that we have created in our model, where we have tested the antitumor impact of a comparatively small number of adoptively transferred γδ T cells in the presence of a much larger number of autologous T cells that are functionally suppressed. Additionally, by performing our studies with a strain of EBV (M81) that produces a mixture of lytic and latent infection (42), rather than the B95-8 laboratory strain that establish mainly latent infection, we have created a more physiologically relevant model where the nature of the viral infection may vary in different anatomical locations. For example, while expression of lytic EBV proteins appears diminished in the spleen compared with tumors (Figure 1E), we have observed dispersed positive staining in the spleen for viral latency proteins such as EBNA1 (data not shown), suggesting that EBV-infected cells in that location may be in a less active state of infection. Interestingly, we have found that in contrast to the effect on tumors, administration of γδ T cells at late time points does not seem to result in reduced frequencies of B cells in the spleen (Supplemental Figure 3). Thus, it appears that the adoptively transferred γδ T cells do not target splenic B cells in this model, despite the presence of latent EBV infection at that location.

It is not clear how the immunotherapeutic Vδ2$^+$ T cells might distinguish between B cells in spleen versus tumor in this model. One mechanism that might explain this is that the tumor B cells may overproduce cellular prenylpyrophosphate compounds (e.g., IPP) that activate Vδ2$^+$ T cells, perhaps as a result of their

more aggressive viral gene expression, compared with EBV-infected B cells in the spleen. This mechanism would be consistent with the observations from our in vitro analyses using U-251 cells (Figure 3B), which suggested that IPP accumulation provides the major signal to activate the cytolytic responses of our immunotherapeutic Vδ2$^+$ T cells. However, we have not determined whether the in vivo antitumor effects of the Vδ2$^+$ T cells involve TCR-mediated recognition, or whether other ligands may be involved that distinguish the tumor B cells from those in the spleen. Similarly, it is not clear whether the effects of the immunotherapeutic γδ T cells in this model are due to direct cytolysis of tumor cells, or to a different mechanism such as cytokine secretion, or even by serving as highly stimulatory antigen-presenting cells (APCs) for HLA-restricted T cells, as reported previously by others (43–46).

Another important caveat to our study is the presence of a contaminating fraction of αβ T cells (typically less than 20%) within the Zometa-expanded T cell cultures that we used for immunotherapies. Our results suggest that these contaminating T cells do not mediate strong effector functions in vivo since they appear not to localize efficiently to the tumor tissue and they show more elevated PD-1 expression (Figures 7 and 8). Additionally, since they are allogeneic to the B cells in this model they might be expected to target those in the spleen as well as the tumors, which we do not observe (Supplemental Figure 3). To confirm the lack of effector responses by conventional T cells, we tested whether we could detect EBV peptide–specific T cell responses from mice that had received the immunotherapeutic cell mixture. As shown in Supplemental Figure 4, we did not observe responses to EBV peptides by T cells harvested from mice that received adoptive therapy, although we did detect a response to anti-CD3 stimulation. Nevertheless, removal of these contaminating T cells is likely to be an important consideration before translation to clinical scenarios.

Phase I clinical trials involving adoptively transferred γδ T cells carried out thus far have yielded somewhat mixed results. Four trials have shown results consistent with an antitumor effect of the therapy. Two were trials involving patients who had advanced renal cell carcinomas; in one, 3 out of 5 patients who received adoptive transfer of aminobisphosphonate-expanded γδ T cells showed delayed tumor doubling time (47), and in the other (a phase I/II trial) all 11 patients who received Zometa-expanded γδ T cells and recombinant IL-2 showed prolonged tumor doubling time (48). In another trial involving 18 subjects with metastatic solid tumors who received adoptive transfer of Zometa-expanded γδ T cells in combination with Zometa and IL-2, three patients showed measurable disease responses (49). Finally, in a trial of 4 patients with advanced hematological malignancies who received haploidentical transplants highly enriched for γδ T cells followed by in vivo administration of Zometa and IL-2, three subjects showed complete remission lasting more than 6 months while one died of an infection 6 weeks after the cell transfusion (50).

In contrast, several other phase I trials, while providing data that γδ T cell adoptive therapy is well tolerated, have not shown clear evidence of antitumor effects. In a trial involving 6 subjects with multiple myeloma who received Zometa-expanded γδ T cells in combination with Zometa and IL-2, four of the subjects showed M protein levels that remained at baseline, but there was no clear correlation between the amount of γδ T cells infused and clinical outcomes (51). In a study of 10 patients with metastatic renal cell carcinoma who received γδ T cells expanded using bromohydrin pyrophosphate and IL-2, six subjects showed stabilized disease but there was no clear antitumor effect (52). Finally, in 2 studies of non–small cell lung cancer involving 10 and 15 patients, respectively, who received Zometa-expanded γδ T cells and IL-2, there were no objective indicators of success although about one-third to one-half of the patients showed stable disease after therapy (53, 54).

What is clear from these published clinical trials is that in addition to variation in the types of cancer treated, there is little consistency in the protocols used to expand γδ T cells in vitro for cellular immunotherapy, or in how the immunotherapy was delivered (e.g., γδ T cells alone, or in combination with activating agents such as IL-2 and Zometa). Our results suggest that in addition to standardizing these factors, it will be important to evaluate PD-1 expression of immunotherapeutic γδ T cells expanded in vitro. Our preclinical model of B lymphomagenesis is thus likely to be highly useful for studies aimed at understanding how to optimize the antitumor effects of human Vδ2$^+$ T cells as agents of cellular immunotherapy, as well as further delineating their activation requirements and mechanisms of action in vivo.

Methods

Preparation of EBV. All experiments were performed using the lytic M81 strain of EBV. M81 bacmid expressing green fluorescent protein (GFP) and a hygromycin B resistance gene was constructed using bacterial artificial chromosome technology as described (42). Infectious viral particles were produced from

293 cell lines that were stably infected with the M81 strain of EBV following transfection with EBV BZLF1 expression vector as previously described (55). The titer of infectious EBV was determined by assessing the number of fluorescent Raji cells derived from serial dilutions of the concentrated virus stock and calculating the green Raji unit (GRU) titer, as previously described (55).

In vivo model. Human umbilical CBMCs were purified by density gradient centrifugation using Ficoll Paque PLUS (GE Healthcare), washed in sterile PBS, followed by 2 low-speed centrifugation spins (200–300 *g*) to remove platelets, and if necessary to diminish red blood cell contamination they were treated briefly with ammonium-chloride-potassium (ACK) lysis buffer. The CBMCs were then suspended in tissue culture medium (RPMI 1640 with L-glutamine [Corning] and supplemented with 10% bovine calf serum [Thermo Fisher Scientific], 3% human AB serum [Atlanta Biologicals], 1% penicillin/streptomycin [Mediatech]) and exposed to 2,000 U of the M81 strain of EBV, or mock treated in medium alone, for 2 hours. Finally, the CBMCs were washed and resuspended in sterile PBS, and 10×10^6 cells per mouse were injected intraperitoneally into 6- to 8-week-old NOD.Cg-Prkdc^{scid}Il2rg^{tm1Wjl}/SzJ (NSG) mice (Jackson Labs). Mice were maintained in a specific pathogen–free facility using sterilized cages, bedding, food, and water, and were euthanized at day 29–30 or when they appeared moribund on the basis of weight loss and body condition score. Grossly visible tumor tissue was carefully excised and weighed, and tissues were harvested for further analysis.

Expansion of Vδ2$^+$ T cells from PBMCs and adoptive transfer into mice. PBMCs were isolated from venous blood samples from healthy donors obtained in accordance with a protocol approved by the University of Wisconsin Minimal Risk IRB. Written informed consent for experimental use of cells was obtained from all donors. Blood was processed by density gradient centrifugation using Ficoll-paque PLUS according to the manufacturer's protocol. To expand Vδ2$^+$ T cells, freshly isolated PBMCs were exposed for 7–14 days to 2.5 μM Zometa (Novartis) and 200 units/ml IL-2, in tissue culture medium that was composed of RPMI 1640 containing L-glutamine, 15% heat-inactivated bovine calf serum (Thermo Fisher Scientific), 3% human AB serum, and 100 μg/ml each of penicillin and streptomycin. The expanded Vδ2$^+$ T cells were washed and resuspended in sterile PBS, then administered intravenously via retro-orbital injection to anesthetized mice at the indicated day. For immunotherapy treatment studies, 5×10^6 to 10×10^6 Vδ2$^+$ T cells per mouse were injected; for tumor infiltration studies, 1×10^6 to 5×10^6 Vδ2$^+$ T cells per mouse were injected.

Generation and analysis of U-251 cells expressing NKG2D ligands. U-251 MG cells (formerly known as U-373 MG cells) stably expressing the NKG2D ligands ULBP1, ULBP2, ULBP3, ULBP4, MICA, or MICB were generated by retroviral transduction using the vector pLNCX (Clontech), as previously described (56). The U-251 parental cells and retroviral transductants were incubated overnight in culture medium (DMEM supplemented with 5% heat-inactivated bovine calf serum, 5% fetal bovine serum, and 100 μg/ml each of penicillin and streptomycin) in the presence or absence of 1.25 μM Zometa. The U-245 cells were washed and combined at a 1:1 ratio with Vδ2$^+$ T cells expanded from PBMCs. After a 6-hour coincubation, the cells were harvested, washed, and Fc receptors were blocked by incubation in PBS containing 20% human AB serum. Cells were stained with antibodies against CD3, Vδ2 TCR, and CD107a (BioLegend; clone OKT3, B6, and H4A3, respectively) or an isotype-matched control monoclonal antibody. Where indicated, intracellular cytokine staining for IFN-γ (BioLegend; clone 4S.B3) was also performed using the BD Cytofix/Cytoperm kit (BD Biosciences).

Histological analyses. Tissues were fixed in 10% buffered formalin and embedded in paraffin prior to sectioning. Sections were deparaffinized and processed for H&E staining, immunohistochemistry, or in situ hybridization. Immunohistochemistry was performed using an antibody against the EBV protein EBNA1 (clone 1EB14, Santa Cruz Biotechnology Inc.), or with the following antibodies against human cellular antigens: CD20 (clone H1, BD-Pharmingen); CD4 (clone 4B12, Leica Microsystems); CD8 (clone SP16, Biocare Medical LLC). Antigen retrieval was performed using Rodent Decloaker (Biocare Medical). Antibody labeling was detected and visualized using a horseradish peroxidase (HRP)-polymer kit with diaminobenzidine (DAB) development (Biocare Medical). EBER detection was performed by in situ hybridization using the PNA ISH Detection Kit (DakoCytomation).

Flow cytometric analysis. Single-cell suspensions were pelleted, washed, and resuspended in PBS containing 15% human AB serum to block Fc receptors. Staining was performed using fluorescently labeled monoclonal antibodies specific for human cell surface markers, and compared to isotype-matched negative control antibodies used for fluorescence minus one (FMO) conditions. The following antibodies used for staining were purchased from BioLegend: anti–HLA-A,B,C (clone W6/32), anti-CD45 (clone HI30), anti-CD3 (clone OKT3), anti-CD4 (clone OKT4), anti-CD8 (clone RPA-T8), anti-CD19 (clone HIB19),

anti-CD20 (clone 2H7), anti–PD-L1 (clone 29E.2A3), anti–PD-L2 (clone 24F.10C12), anti–PD-1 (clone EH12.2H7), anti-CD69 (clone FN50), anti-NKG2D (clone 1D11), anti-BTN3A1 (clone BT3.1), anti-MICA/B (clone 6D4), and anti-Vδ2 (clone B6). Additionally, the following monoclonal antibodies were purchased from R&D Systems: anti-ULBP1 (clone 170818), anti-ULBP2/5/6 (clone 165903), anti-ULBP3 (clone 166510), and anti-ULBP4 (clone 709116). Compensation was performed using single-color controls, and staining was detected using an LSRII flow cytometer (BD Biosciences). Flow cytometric data were analyzed using FlowJo software v9.3.1 (Tree Star).

Statistics. Experimental datasets that consisted of independent analyses of individual mice were analyzed using a 2-tailed, nonparametric *t* test (Mann-Whitney analysis); datasets that consisted of replicate analyses of samples from the same mouse were analyzed using an unpaired, 2-tailed parametric *t* test. For datasets where treatment groups from independent experiments were aggregated, statistical analysis was performed using the van Elteren test to account for the effect of stratification. *P* values of 0.05 or less were considered significant.

Study approval. Experimental protocols involving animals were approved by the University of Wisconsin-Madison IACUC, and work involving animals was conducted in accordance with the NIH Guide for the care and use of laboratory animals. Deidentified human umbilical CBMCs were obtained from the University of Colorado Cord Blood Bank, and analyzed according to an IRB protocol approved by the University of Wisconsin Minimal Risk IRB.

Author contributions

JEG designed the research studies, wrote the manuscript, and prepared figures. NAZ, AS, XX,and SM conducted experiments and acquired data. NAZ, AGF, and JEG analyzed and interpreted data. JRM, SCK, CLS, and AWH provided critical reagents.

Acknowledgments

Primary funding for this work was provided by a pilot grant from the University of Wisconsin Carbone Cancer Center that was supported in part by NIH grant NCI P30 CA014520. Additional funding was provided by the following NIH grants: R21 AI116007 to JEG; R21 AI105847 and R01 AI069099 to AWH; R01 CA174462 and P01-CA022443 to SCK; support from T32 CA157322 for NAZ. The funders had no role in study design, data collection and analysis, decision to publish, or preparation of the manuscript.

Address correspondence to: Jenny E. Gumperz, Department of Medical Microbiology and Immunology, University of Wisconsin School of Medicine and Public Health, Microbial Sciences Building, Room 4305, 1550 Linden Dr., Madison, Wisconsin 53706, USA. Phone: 608.263.6902; Email: jegumperz@wisc.edu.

SM's present address is: Sanofi, Inc., Cambridge, Massachusetts, USA.

CLS's present address is: Carroll University, Waukesha, Wisconsin, USA.

1. Moingeon P, et al. A unique T-cell receptor complex expressed on human fetal lymphocytes displaying natural-killer-like activity. *Nature*. 1986;323(6089):638–640.
2. Sturm E, Braakman E, Fisch P, Vreugdenhil RJ, Sondel P, Bolhuis RL. Human V gamma 9-V delta 2 T cell receptor-gamma delta lymphocytes show specificity to Daudi Burkitt's lymphoma cells. *J Immunol*. 1990;145(10):3202–3208.
3. Fisch P, et al. Gamma/delta T cell clones and natural killer cell clones mediate distinct patterns of non-major histocompatibility complex-restricted cytolysis. *J Exp Med*. 1990;171(5):1567–1579.
4. Ensslin AS, Formby B. Comparison of cytolytic and proliferative activities of human gamma delta and alpha beta T cells from peripheral blood against various human tumor cell lines. *J Natl Cancer Inst*. 1991;83(21):1564–1569.
5. Strid J, et al. Acute upregulation of an NKG2D ligand promotes rapid reorganization of a local immune compartment with pleiotropic effects on carcinogenesis. *Nat Immunol*. 2008;9(2):146–154.
6. Liu Z, Eltoum IE, Guo B, Beck BH, Cloud GA, Lopez RD. Protective immunosurveillance and therapeutic antitumor activity of gammadelta T cells demonstrated in a mouse model of prostate cancer. *J Immunol*. 2008;180(9):6044–6053.
7. Ma C, et al. Tumor-infiltrating γδ T lymphocytes predict clinical outcome in human breast cancer. *J Immunol*. 2012;189(10):5029–5036.
8. Coffelt SB, et al. IL-17-producing γδ T cells and neutrophils conspire to promote breast cancer metastasis. *Nature*. 2015;522(7556):345–348.
9. De Libero G. Tissue distribution, antigen specificity and effector functions of gamma delta T cells in human diseases. *Springer*

Semin Immunopathol. 2000;22(3):219–238.
10. Fisher JP, et al. Neuroblastoma killing properties of Vδ2 and Vδ2-negative γδT cells following expansion by artificial antigen-presenting cells. *Clin Cancer Res*. 2014;20(22):5720–5732.
11. Vavassori S, et al. Butyrophilin 3A1 binds phosphorylated antigens and stimulates human γδ T cells. *Nat Immunol*. 2013;14(9):908–916.
12. Wang H, et al. Butyrophilin 3A1 plays an essential role in prenyl pyrophosphate stimulation of human Vγ2Vδ2 T cells. *J Immunol*. 2013;191(3):1029–1042.
13. Sandstrom A, et al. The intracellular B30.2 domain of butyrophilin 3A1 binds phosphoantigens to mediate activation of human Vγ9Vδ2 T cells. *Immunity*. 2014;40(4):490–500.
14. Wang H, Morita CT. Sensor function for butyrophilin 3A1 in prenyl pyrophosphate stimulation of human Vγ2Vδ2 T cells. *J Immunol*. 2015;195(10):4583–4594.
15. Rhodes DA, et al. Activation of human γδ T cells by cytosolic interactions of BTN3A1 with soluble phosphoantigens and the cytoskeletal adaptor periplakin. *J Immunol*. 2015;194(5):2390–2398.
16. Riaño F, et al. Vγ9Vδ2 TCR-activation by phosphorylated antigens requires butyrophilin 3 A1 (BTN3A1) and additional genes on human chromosome 6. *Eur J Immunol*. 2014;44(9):2571–2576.
17. Tanaka Y, Morita CT, Tanaka Y, Nieves E, Brenner MB, Bloom BR. Natural and synthetic non-peptide antigens recognized by human gamma delta T cells. *Nature*. 1995;375(6527):155–158.
18. Gober HJ, Kistowska M, Angman L, Jenö P, Mori L, De Libero G. Human T cell receptor gammadelta cells recognize endogenous mevalonate metabolites in tumor cells. *J Exp Med*. 2003;197(2):163–168.
19. Champsaur M, Lanier LL. Effect of NKG2D ligand expression on host immune responses. *Immunol Rev*. 2010;235(1):267–285.
20. Lanier LL. NKG2D receptor and its ligands in host defense. *Cancer Immunol Res*. 2015;3(6):575–582.
21. Das H, et al. MICA engagement by human Vgamma2Vdelta2 T cells enhances their antigen-dependent effector function. *Immunity*. 2001;15(1):83–93.
22. Bauer S, et al. Activation of NK cells and T cells by NKG2D, a receptor for stress-inducible MICA. *Science*. 1999;285(5428):727–729.
23. Rincon-Orozco B, Kunzmann V, Wrobel P, Kabelitz D, Steinle A, Herrmann T. Activation of V gamma 9V delta 2 T cells by NKG2D. *J Immunol*. 2005;175(4):2144–2151.
24. Chitadze G, Bhat J, Lettau M, Janssen O, Kabelitz D. Generation of soluble NKG2D ligands: proteolytic cleavage, exosome secretion and functional implications. *Scand J Immunol*. 2013;78(2):120–129.
25. Pang DJ, Neves JF, Sumaria N, Pennington DJ. Understanding the complexity of γδ T-cell subsets in mouse and human. *Immunology*. 2012;136(3):283–290.
26. Afrache H, Gouret P, Ainouche S, Pontarotti P, Olive D. The butyrophilin (BTN) gene family: from milk fat to the regulation of the immune response. *Immunogenetics*. 2012;64(11):781–794.
27. Malkovska V, Cigel FK, Armstrong N, Storer BE, Hong R. Antilymphoma activity of human gamma delta T-cells in mice with severe combined immune deficiency. *Cancer Res*. 1992;52(20):5610–5616.
28. Chen J, Niu H, He W, Ba D. Antitumor activity of expanded human tumor-infiltrating gammadelta T lymphocytes. *Int Arch Allergy Immunol*. 2001;125(3):256–263.
29. Zheng BJ, et al. Anti-tumor effects of human peripheral gammadelta T cells in a mouse tumor model. *Int J Cancer*. 2001;92(3):421–425.
30. Lozupone F, et al. Effect of human natural killer and gammadelta T cells on the growth of human autologous melanoma xenografts in SCID mice. *Cancer Res*. 2004;64(1):378–385.
31. Kabelitz D, Wesch D, Pitters E, Zöller M. Characterization of tumor reactivity of human V gamma 9V delta 2 gamma delta T cells in vitro and in SCID mice in vivo. *J Immunol*. 2004;173(11):6767–6776.
32. Xiang Z, et al. Targeted activation of human Vγ9Vδ2-T cells controls Epstein-Barr virus-induced B cell lymphoproliferative disease. *Cancer Cell*. 2014;26(4):565–576.
33. Vereide D, Sugden B. Insights into the evolution of lymphomas induced by Epstein-Barr virus. *Adv Cancer Res*. 2010;108:1–19.
34. Ma SD, et al. LMP1-deficient Epstein-Barr virus mutant requires T cells for lymphomagenesis. *J Clin Invest*. 2015;125(1):304–315.
35. Ma SD, et al. PD-1/CTLA-4 blockade inhibits Epstein-Barr virus-induced lymphoma growth in a cord blood humanized-mouse model. *PLoS Pathog*. 2016;12(5):e1005642.
36. Zumwalde NA, et al. Analysis of immune cells from human mammary ductal epithelial organoids reveals Vδ2$^+$ T cells that efficiently target breast carcinoma cells in the presence of bisphosphonate. *Cancer Prev Res (Phila)*. 2016;9(4):305–316.
37. Bukowski JF, Morita CT, Band H, Brenner MB. Crucial role of TCR gamma chain junctional region in prenyl pyrophosphate antigen recognition by gamma delta T cells. *J Immunol*. 1998;161(1):286–293.
38. Bukowski JF, Morita CT, Tanaka Y, Bloom BR, Brenner MB, Band H. V gamma 2V delta 2 TCR-dependent recognition of non-peptide antigens and Daudi cells analyzed by TCR gene transfer. *J Immunol*. 1995;154(3):998–1006.
39. Prabhu SB, et al. Comparison of human neonatal and adult blood leukocyte subset composition phenotypes. *PLoS One*. 2016;11(9):e0162242.
40. Schildberg FA, Klein SR, Freeman GJ, Sharpe AH. Coinhibitory pathways in the B7-CD28 ligand-receptor family. *Immunity*. 2016;44(5):955–972.
41. Leung J, Suh WK. The CD28-B7 family in anti-tumor immunity: emerging concepts in cancer immunotherapy. *Immune Netw*. 2014;14(6):265–276.
42. Tsai MH, et al. Spontaneous lytic replication and epitheliotropism define an Epstein-Barr virus strain found in carcinomas. *Cell Rep*. 2013;5(2):458–470.
43. Brandes M, Willimann K, Moser B. Professional antigen-presentation function by human gammadelta T cells. *Science*. 2005;309(5732):264–268.
44. Landmeier S, et al. Activated human gammadelta T cells as stimulators of specific CD8$^+$ T-cell responses to subdominant Epstein Barr virus epitopes: potential for immunotherapy of cancer. *J Immunother*. 2009;32(3):310–321.
45. Brandes M, et al. Cross-presenting human gammadelta T cells induce robust CD8$^+$ alphabeta T cell responses. *Proc Natl Acad Sci*

U S A. 2009;106(7):2307–2312.
46. Altvater B, et al. Activated human γδ T cells induce peptide-specific $CD8^+$ T-cell responses to tumor-associated self-antigens. *Cancer Immunol Immunother*. 2012;61(3):385–396.
47. Kobayashi H, et al. Safety profile and anti-tumor effects of adoptive immunotherapy using gamma-delta T cells against advanced renal cell carcinoma: a pilot study. *Cancer Immunol Immunother*. 2007;56(4):469–476.
48. Kobayashi H, Tanaka Y, Yagi J, Minato N, Tanabe K. Phase I/II study of adoptive transfer of γδ T cells in combination with zoledronic acid and IL-2 to patients with advanced renal cell carcinoma. *Cancer Immunol Immunother*. 2011;60(8):1075–1084.
49. Nicol AJ, et al. Clinical evaluation of autologous gamma delta T cell-based immunotherapy for metastatic solid tumours. *Br J Cancer*. 2011;105(6):778–786.
50. Wilhelm M, et al. Successful adoptive transfer and in vivo expansion of haploidentical γδ T cells. *J Transl Med*. 2014;12:45.
51. Abe Y, et al. Clinical and immunological evaluation of zoledronate-activated Vgamma9gammadelta T-cell-based immunotherapy for patients with multiple myeloma. *Exp Hematol*. 2009;37(8):956–968.
52. Bennouna J, et al. Phase-I study of Innacell gammadelta, an autologous cell-therapy product highly enriched in gamma9delta2 T lymphocytes, in combination with IL-2, in patients with metastatic renal cell carcinoma. *Cancer Immunol Immunother*. 2008;57(11):1599–1609.
53. Nakajima J, et al. A phase I study of adoptive immunotherapy for recurrent non-small-cell lung cancer patients with autologous gammadelta T cells. *Eur J Cardiothorac Surg*. 2010;37(5):1191–1197.
54. Sakamoto M, et al. Adoptive immunotherapy for advanced non-small cell lung cancer using zoledronate-expanded γδTcells: a phase I clinical study. *J Immunother*. 2011;34(2):202–211.
55. Ma SD, et al. A new model of Epstein-Barr virus infection reveals an important role for early lytic viral protein expression in the development of lymphomas. *J Virol*. 2011;85(1):165–177.
56. Schneider CL, Hudson AW. The human herpesvirus-7 (HHV-7) U21 immunoevasin subverts NK-mediated cytoxicity through modulation of MICA and MICB. *PLoS Pathog*. 2011;7(11):e1002362.